

# Valley-orbital splitting of the ground state of acceptor-bound excitons in silicon

M. V. Gorbunov, A. S. Kaminski, and A. N. Safonov

*Institute of Radio Engineering and Electronics, USSR Academy of Sciences*

(Submitted 19 June 1987)

Zh. Eksp. Teor. Fiz. **94**, 247–258 (February 1988)

We have investigated the spectrum of recombination radiation arising from phononless radiative decay of excitons bound to impurity atoms of gallium, aluminum, and indium in single-crystal silicon in the temperature interval 2 to 20 K. By analyzing the spectral intensity distribution and polarization of the recombination radiation in samples subjected to uniaxial stress, we have determined the magnitude and sign of the constant which characterizes valley-orbital splitting of the ground state of excitons bound to atoms of gallium and aluminum; we have also found the constants which determine the relative probability of phononless radiative recombination, along with the deformation potential constants  $b'$  and  $d'$  for the ground state of holes bound to gallium ions. We observed that as the sample temperature decreases the luminescence line of excitons bound to impurity atoms from the III and V groups is broadened.

## 1. INTRODUCTION

Valley-orbital splitting (VOS) of electron states localized at shallow impurity centers is presented only in multi-valley semiconductors. The electron wave functions in such semiconductors are linear combinations of single-valley electron states which satisfy symmetry conditions; these linear combinations arise because of intervalley electron scattering by the potential due to an impurity center. Although this phenomenon is well-known and well-studied for electrons bound to donor impurity centers,<sup>1)</sup> it remains almost unstudied for electrons which take part in multiparticle electron-impurity complexes (MEICs) at impurities of acceptor type. This is not surprising, because in this case the VOS is approximately two orders of magnitude smaller than the VOS for donor impurities, amounting to  $40 \mu\text{eV}$  (Ref. 1) and  $70 \mu\text{eV}$  (Ref. 3) for excitons bound to impurity atoms of boron and aluminum, respectively. We note that in investigating such small splittings it is necessary not only to have spectroscopic equipment with a resolution of  $\sim 10 \mu\text{eV}$ , but also to have sample crystals which are free of internal mechanical stresses.

This paper is devoted to an investigation of recombination radiation (RR) arising from phononless radiative decay of excitons bound to impurity atoms of gallium, aluminum and indium in silicon. The ground state energy of an exciton bound to these impurities is lower than the excited-state energies by more than 1 meV, so that transitions to the ground state form rather sharp lines in the luminescence spectrum; for this reason, our attention will center primarily on investigation of VOS.

## 2. EXPERIMENTAL METHOD

We investigated oxygen-free single-crystal silicon with gallium ( $N_{\text{Ga}} = 2 \times 10^{14}$  to  $7 \times 10^{15} \text{ cm}^{-3}$ ), aluminum ( $N_{\text{Al}} = 2 \times 10^{14} \text{ cm}^{-3}$ ) and indium ( $N_{\text{In}} = 7 \times 10^{15} \text{ cm}^{-3}$ ) impurities, obtained by the method of crucibleless zone refining. The samples were cut along the [001] and [111] crystal axes. The crystals were oriented in the [111] direction to an accuracy within  $10'$ . The sample temperature could be varied smoothly from 2 to 20 K and was measured using a thermistor placed on the lateral face of the sample. The samples were excited by radiation from an LG-106M-1

argon laser. The setup for applying uniaxial compression to the samples and the apparatus for spectroscopic analysis and recording the RR was described in Ref. 4.

## 3. SPECTRUM OF RECOMBINATION RADIATION

In Fig. 1 we show the phononless part of the RR spectrum, which arises from radiative decay of excitons bound to gallium impurity atoms (BEs); excitons bound to aluminum and indium impurity atoms have analogous spectra in silicon.<sup>1,3</sup> There are three well-marked luminescence bands in the spectrum:  $\alpha$ ,  $\beta$ , and  $\gamma$ . The  $\alpha$  band is observed both at low and at high temperatures, and corresponds to ground-state decay of BEs. The  $\beta$  and  $\gamma$  bands appear only at high temperatures ( $\sim 10 \text{ K}$ ) and correspond to decay of BEs in excited states. The origin of the ground-state and excited-state BEs is well-known, and is related to interaction of the holes in the BE.<sup>1,3</sup> We note, however, an interesting fact which has not been reported by other investigators: as the temperature rises to 10-15 K, the  $\alpha$ -NP luminescence band from excitons bound to impurity atoms of gallium, aluminum and indium is significantly broadened and loses its structure (see the half-width of the  $\alpha$ -NP band in Figs. 1 and 2). The  $\alpha_1$ -NP lines, which are due to excitons bound on impurity atoms of phosphorous and arsenic, are also broadened; however, this broadening becomes appreciable only at higher tempera-

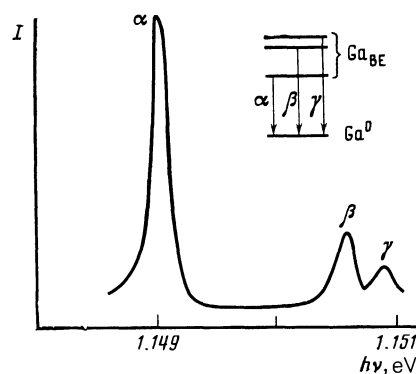


FIG. 1. Spectral distribution of the  $\alpha$ ,  $\beta$ , and  $\gamma$ -NP components of the luminescence of excitons bound to impurity atoms of gallium ( $N_{\text{Ga}} = 7 \times 10^{14} \text{ cm}^{-3}$ ) in silicon at  $T = 10 \text{ K}$ . The spectral resolution is  $45 \mu\text{eV}$ ; the width at half-maximum is  $160 \mu\text{eV}$ .

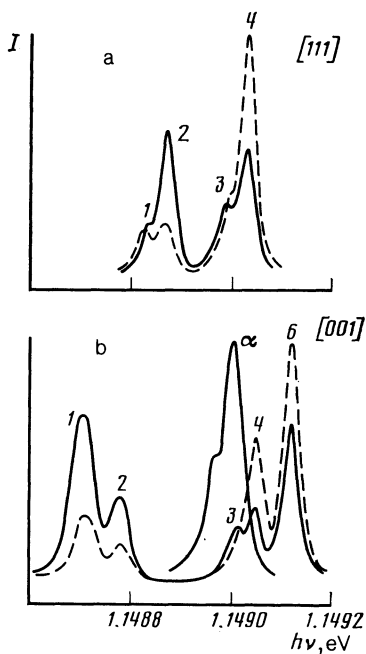


FIG. 2. Spectral distribution of the  $\alpha$ -NP components of the luminescence of excitons bound to impurity atoms of gallium at  $T = 4.2$  K. The luminescence is polarized parallel (dotted curves) and perpendicular (continuous curves) to the deformation axis: a)  $P = 8$  MPa in the [111] direction; the spectral resolution is  $23 \mu\text{eV}$ ; b)  $P = 5$  MPa in the [001] direction; the spectral resolution is  $23 \mu\text{eV}$ . The spectrum corresponding to  $P = 0$  was obtained with a spectral resolution of  $12 \mu\text{eV}$ .

tures (compared to excitons bound on neutral acceptors). At this time it is still unclear whether the observed broadening of the RR lines is connected with the finite lifetime of the ground state of BEs or with fluctuations in the central-cell potentials.

In what follows we limit ourselves to investigating  $\alpha$ -NP luminescence bands from excitons bound to impurity atoms of gallium, aluminum and indium. The spectra of these bands were taken at 4.2 K with sufficient resolution to observe their structure. In Figs. 2 and 4 (see below) we also give RR spectra of excitons in crystals subjected to uniaxial stress in the [111] and [001] directions. The continuous and dotted curves correspond to RR polarized perpendicular and parallel to the direction of strain. The dependence of the spectral position of the various components of the spectrum (denoted in Fig. 2 by figures) on applied stress for excitons bound to impurity atoms of gallium is shown in Fig. 3. The inset in Fig. 3 shows the behavior of these luminescence components in the low-stress region on a larger scale.

Before we proceed to more detailed analysis of the RR spectra, let us give a general picture of the phenomena we observe. For the present we will not take into account the structure of the  $\alpha$ -NP luminescence band, which as we will show below, is connected with VOS of the BE ground state; instead we will limit ourselves to studying excitons bound to gallium atoms. The  $\alpha$  luminescence band which we studied arises from the radiative decay of BEs from the ground state, to which corresponds a two-hole wave function which transforms according to the unit  $\Gamma_1$  representation. For this reason, the splitting of terms of the BE ground state under uniaxial strain can take place only because of splitting of the electronic BE state. The final state for radiative decay of a BE is a neutral acceptor, whose wave function transforms

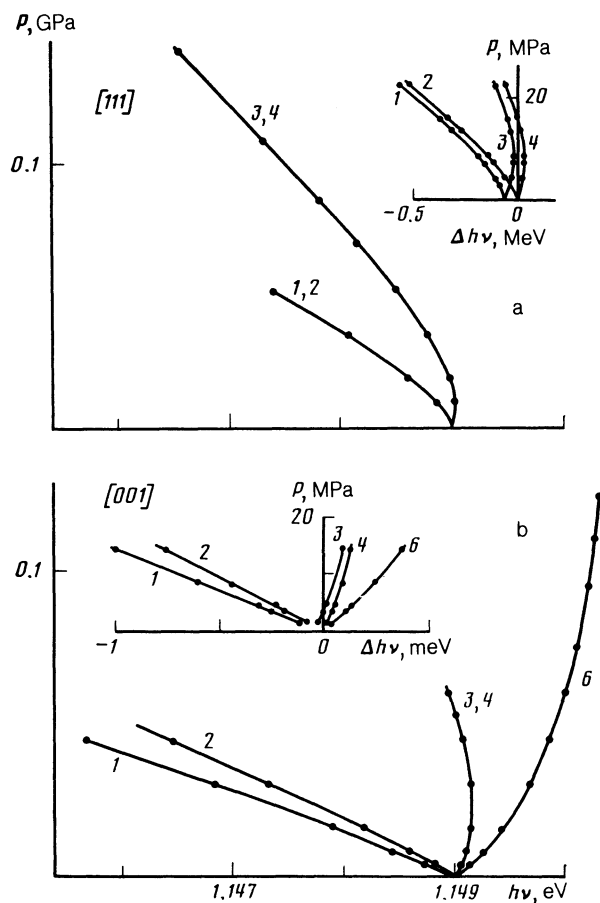


FIG. 3. Dependence of the spectral position of the  $\alpha$ -NP luminescence components of excitons bound to impurity atoms of gallium in silicon on the magnitude of the applied stress. In the inset we give these dependences in the region of small stresses on a smaller scale. The numbers on the curves are related to the corresponding components of the luminescence shown in Fig. 2(a) for  $P \parallel [111]$ , 2(b)  $P \parallel [001]$ .

according to the irreducible representation  $\Gamma_e$ . Therefore, under uniaxial compression of the crystal, the final state is always split in two. For compression along the [111] and [001] directions, the magnitude of this splitting equals  $(d'/\sqrt{3})S_{44}P$  and  $2b'(S_{11} - S_{12})P$ , where  $S_{44} = 1.256 \times 10^{-11} \text{ Pa}^{-1}$ ,  $S_{11} = 0.768 \times 10^{-11} \text{ Pa}^{-1}$ ,  $S_{12} = -0.214 \times 10^{-11} \text{ Pa}^{-1}$ ;  $b'$  and  $d'$  are the deformation potential constants of the BE ground state,  $P$  is the stress.

Thus, for compression in the [111] direction the initial state of the BE is not split, and the observed splitting is connected with splitting of the final state (i.e., the acceptor). The magnitude of this splitting equals the energy difference between the photons corresponding to peaks 2 and 4 or 1 and 3 of Fig. 2a. Furthermore, the absence of effective thermalization of the charges is a further indication that this splitting is actually connected with the splitting of the final state. When the samples are compressed in the [001] direction, in addition to the final-state splitting there is also a splitting in the initial state, which, as we have already noted, can occur only because of the electron terms. The magnitude of this splitting equals the energy difference corresponding to peaks 1 and 4 or 2 and 6 of Figs. 2b and 3b. The magnitude of the final-state splitting in this case is given by the energy difference corresponding to peaks 1 and 2 or 4 and 6 of these same figures. We note that here the intensity of peaks 3, 4, and 6

relative to the upper electron valley is practically unchanged, a result easily explained by the large intervalley transfer time<sup>1</sup> in BEs compared to their lifetime, which equals  $3 \times 10^{-8}$  sec (Ref. 5). We recall that BEs which are associated with the upper valleys are customarily referred to as "hot".

At this point we interrupt the discussion with yet another fact. As is clear from Fig. 3, the magnitudes of the shifts of the individual lines depend nonlinearly on stress: as the stress increases lines 1 and 2 disappear gradually from the RR spectrum when  $P \parallel [111]$ , while lines 1, 3, 4 do the same when  $P \parallel [001]$ . Both of these phenomena are easily explained by the interaction of the ground and excited states of the BE. Actually, as the magnitude of the stress increases the contribution of the two-particle hole state  $|\pm 3/2\rangle$  to BE ground state increases, while that of the state  $|-3/2\rangle|3/2\rangle$  decreases: for this reason, radiative decays of BEs which result in acceptors appearing in states with momentum  $\pm 3/2$  become forbidden. Despite the nonlinear character of the stress dependence of the shift in spectral position of the individual RR lines (see Ref. 3), the magnitude of the splitting of the acceptor levels, as is not hard to verify, depends linearly on stress. This allows us to determine the deformation potential constants  $b'$  and  $d'$  for the ground state of excitons bound to gallium atoms. These constants determine the splitting of the acceptor ground state for an arbitrary uniaxial deformation, and equal  $-0.9$  and  $-3.0$  eV.

In concluding this section we recall that "hot" BE luminescence and the disappearance of the individual components of the RR spectrum for uniaxially compressed samples was observed earlier for the case of excitons bound on aluminum atoms in silicon.<sup>1</sup> For this reason we limit ourselves to a short description of these phenomena.

#### 4. ANALYSIS OF THE EXPERIMENTAL RESULTS

It was noted earlier that the structure of the  $\alpha$  band is determined by VOS of the BE terms. This assertion becomes more plausible if we note that for samples compressed along the  $[111]$  direction, which does not cause splitting of the electron terms, the characteristic form of the luminescence bands corresponding to the various final states in many respects recalls the form of the original bands (see Fig. 2a and 4). The spectra obtained from samples compressed along the  $[001]$  direction also point to the reasonableness of this conjecture. However, taken as a whole, the intensity and polarization distributions of the RR spectrum cannot be understood by proceeding only from qualitative arguments. In order to obtain more concrete information on the VOS of the BE terms, we carried out a detailed analysis of the RR spectrum based on symmetry theory. Summarizing this analysis, we found the magnitudes and signs of the constants which determine the VOS for excitons bound to atoms of gallium and aluminum in silicon. As an example, in Fig. 5 we give the ground-state splitting which we obtained from calculations for excitons bound to gallium atoms, and the evolution of this splitting for samples compressed in the  $[111]$  and  $[001]$  directions. The scheme presented in Fig. 5 is found to be in good agreement with all the experimental data available to us.

In our calculations, we used a deliberately simplified model of the exciton bound to atoms of gallium, aluminum and indium in silicon. We assumed that the hole part of the

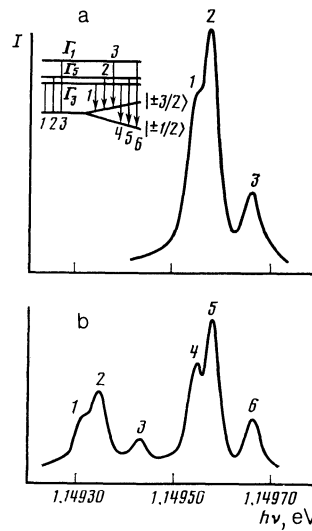


FIG. 4. Spectral distribution of the  $\alpha$ -NP components of the luminescence of excitons bound to impurity atoms of aluminum in silicon ( $N_{Al} = 2 \times 10^{14}$  cm<sup>-3</sup>) at  $T = 4.2$  K. The spectral resolution is  $45 \mu\text{eV}$ , and  $P$  is parallel to  $[111]$ ; a)  $P = 0$ , b)  $P = 17.6$  MPa. In the inset we show the level scheme due to VOS for excitons bound to aluminum atoms.

wave function for the ground state of the bound exciton is given by two-hole antisymmetrized functions of the form

$$\langle r_1, r_2 | \Gamma_1^{2h}; 0 \rangle = \frac{1}{2\sqrt{2}} \left\{ \sum_m \varphi_m(r_1) \hat{K} \psi_m(r_2) - [r_1 \leftrightarrow r_2] \right\}. \quad (1)$$

This function transforms according to the unit representation  $\Gamma_1$  and describes BE states with zero angular momentum. In (1) the functions  $\varphi_m$  and  $\psi_m$  ( $m = \pm 1/2, \pm 3/2$ ) transform under the action of the symmetry operations just like the functions of the canonical basis  $|m\rangle$  (Ref. 4);  $\psi_m$  is close to the corresponding acceptor wave function  $\psi_m^A$ , while  $\varphi_m$  is somewhat more extended;  $\hat{K}$  is the operator for time inversion. Such wave functions only partially take into account the correlation in the hole motion, and can be used for small stresses, where the mixing of the ground and excited states of the BE can be neglected. We also assume that the sixfold valley degeneracy of the BE electrons state is split under the action of the central-cell potential into three states:  $\Gamma_1^e$ ,  $\Gamma_3^e$ , and  $\Gamma_5^e$ , which vary like the ordinary donor states when stress is applied to the crystal.<sup>1</sup> Taking spin into

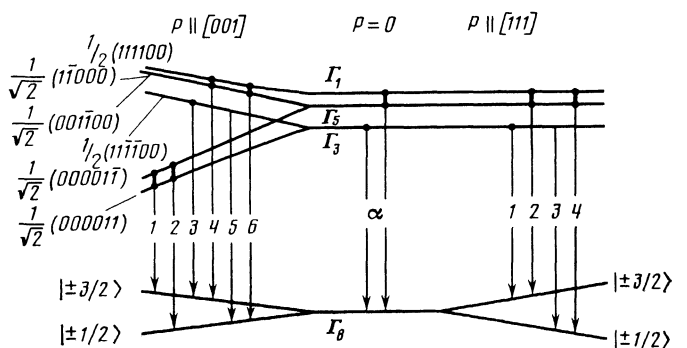


FIG. 5. VOS level scheme for excitons bound to atoms of gallium in crystalline silicon which demonstrates the evolution of VOS for deformation of the crystal along the  $[111]$  and  $[001]$  directions. The numbers on the arrows which denote the various optical transitions correspond to the RR maxima in Fig. 2.

TABLE I. Selection rules for  $|\Gamma_i^e, S_z^e\rangle$  electrons and  $|m\rangle$  holes.

$m$	$S_z^e$	$\Gamma_i^e$					
		$\frac{1}{\sqrt{2}}$ (000011)	$\frac{1}{\sqrt{2}}$ (00001 $\bar{1}$ )	$\frac{1}{\sqrt{2}}$ (1 $\bar{1}$ 0000)	$\frac{1}{\sqrt{2}}$ (001 $\bar{1}$ 00)	$\frac{1}{2}$ (111100)	$\frac{1}{2}$ (11 $\bar{1}$ $\bar{1}$ 00)
$\frac{3}{2}$	$-\frac{1}{2}$	$\sqrt{2}\eta e_+$	$-\sqrt{2}\gamma e_-$	$-\gamma e_z$	$i\gamma e_z$	$(\eta + \lambda) e_+$	$-(\eta - \lambda) e_-$
	$\frac{1}{2}$	$i\sqrt{2/3}\eta e_+$	$-i\sqrt{2/3}\gamma e_-$	$-i\sqrt{1/3}\gamma e_z$	$-\sqrt{3}\gamma e_z$	$(i/\sqrt{3}) \times (\eta + \lambda) e_+$	$(-i/\sqrt{3}) \times (\eta - \lambda) e_-$
$-\frac{1}{2}$	$-\frac{1}{2}$	$(2i/\sqrt{3})\lambda e_z$	0	$(-2/\sqrt{3})\gamma e_y$	$(-2/\sqrt{3})\gamma e_x$	$(4i/\sqrt{6})\eta e_z$	0
	$\frac{1}{2}$	$(-2/\sqrt{3})\lambda e_z$	0	$(-2i/\sqrt{3})\gamma e_y$	$(-2i/\sqrt{3})\gamma e_x$	$(-4/\sqrt{6})\eta e_z$	0
$-\frac{3}{2}$	$-\frac{1}{2}$	$\sqrt{2}\eta e_-$	$\sqrt{2}\gamma e_+$	$\sqrt{1/3}\gamma e_z$	$(i/\sqrt{3})\gamma e_z$	$(1/\sqrt{3}) \times (\eta + \lambda) e_-$	$(-1/\sqrt{3}) \times (\eta - \lambda) e_+$
	$\frac{1}{2}$	$i\sqrt{2}\eta e_-$	$i\sqrt{2}\gamma e_+$	$i\gamma e_z$	$-\gamma e_z$	$i(\eta + \lambda) e_-$	$-i(\eta - \lambda) e_+$

Notation.  $e_+ = (e_x + ie_y)/\sqrt{2}$ ,  $e_- = (e_x - ie_y)/\sqrt{2}$ , where  $e_x$ ,  $e_y$ , and  $e_z$  are components of the polarization vector of the RR. The Z-axis is directed along the [001].

account, we will write these states in the form  $|\Gamma_i^e, S_z^e\rangle$ .

For phononless radiative decay of a BE<sup>2)</sup> which is a consequence of annihilation of an electron and hole in the BE, a neutral acceptor results along with a photon. The probability of such decays is determined by the matrix elements  $\langle \psi_i^A | \hat{U} | BE \rangle$  ( $\hat{U}$  is the interaction operator for BEs with radiation, while  $|BE\rangle = |\Gamma_1^{2h}, 0\rangle |\Gamma_i^e, S_z^e\rangle$  is the BE wave function), which can be calculated in the approximation under discussion here by using the selection rules given in Ref. 1 for phononless radiative decays of excitons in silicon.

The calculations we have carried out for the relative probabilities for decays of excitons bound on acceptors can by convention be divided into two parts. First we calculate the relative probability amplitude for annihilation of an electron whose wave function is a linear combination of single-valley electron wave functions and a hole in the state  $|m\rangle$ . The expressions for the relative probability of such transitions, which is a function of the  $\lambda$ ,  $\eta$  and  $\gamma$  which characterize the phononless radiative decay of excitons, are represented in Table I. In the tables and figures we have used standard

notations for the multielectron wave functions.<sup>1</sup> The linear combinations of electron single-valley states in Table I form a complete basis, i.e., any other combination can be built up from the those presented in the first row of Table I. This table is useful to analyzing the phononless radiative decay of excitons bound both to donors and to acceptors in silicon. Using Table I, we then investigated the relative probability for various phononless radiative decays of excitons bound on acceptors. The expressions for the relative decay probabilities for BEs when the crystal is compressed along the [001] and [111] directions are presented in Tables II and III respectively. In the calculations it was assumed that when the samples are uniaxially deformed (for small stresses) the hole part of the BE wave function (1) remains unchanged, while the electron part changes like a normal donor (see the energy level scheme in Fig. 5). For the final state functions we used the wave functions of an acceptor in an uniaxially-deformed crystal:

$$|\psi_{i,2}^A\rangle = |\pm^{1/2}\rangle, \quad |\psi_{i,4}^A\rangle = |\pm^{3/2}\rangle \quad (2)$$

TABLE II. Relative probability for the radiative transitions  $|\Gamma_1^{2h}, 0\rangle |\Gamma_i^e, S_z^e\rangle \rightarrow \psi_i^A$  in samples compressed along [001].

$\Gamma_i^e$	$\psi_i^A$			
	$\pm^{3/2}, e_{\parallel}$	$\pm^{3/2}, e_{\perp}$	$\pm^{1/2}, e_{\parallel}$	$\pm^{1/2}, e_{\perp}$
$\frac{1}{\sqrt{2}}$ (000011)	0	$2\eta'^2$	$8/3 \lambda'^2$	$2/3 \eta'^2$
$\frac{1}{\sqrt{2}}$ (00001 $\bar{1}$ )	0	$2\gamma'^2$	0	$2/3 \gamma'^2$
$\frac{1}{\sqrt{2}}$ (1 $\bar{1}$ 0000)	$2\gamma'^2$	0	$2/3 \gamma'^2$	0
$\frac{1}{\sqrt{2}}$ (001 $\bar{1}$ 00)	$2\gamma'^2$	0	$2/3 \gamma'^2$	$8/3 \gamma'^2$
$\frac{1}{2}$ (111100)	0	$(\lambda' + \eta')^2$	$16/3 \eta'^2$	$1/3 (\lambda' + \eta')^2$
$\frac{1}{2}$ (11 $\bar{1}$ $\bar{1}$ 00)	0	$(-\lambda' + \eta')^2$	0	$1/3 (\eta' - \lambda')^2$

Remark.  $e_{\perp}$  and  $e_{\parallel}$  are the polarization vectors for RR directed perpendicular and parallel to [001];  $\eta' = A\eta_{\varphi} + B\eta_{\psi}$ , where  $B = \langle \psi_i^A | \varphi_i \rangle$  and  $A = \langle \psi_i^A | \psi_i \rangle$  are overlap integrals of the hole orbitals;  $\eta_{\varphi}, \eta_{\psi}$  are constants introduced in Table I corresponding to the hole functions  $\varphi_m$  and  $\psi_m$ . The expressions for  $\lambda'$  and  $\gamma'$  are determined analogously to  $\eta'$ .

TABLE III. Relative probability for the radiative transitions  $|\Gamma_i^{2A}, 0\rangle|\Gamma_i^e, S_i^e\rangle \rightarrow \psi_i^A$  for samples compressed along [111].

$\Gamma_i^e$	$\psi_i^A$			
	$\pm 3/2, e_{\parallel}$	$\pm 3/2, e_{\perp}$	$\pm 1/2, e_{\parallel}$	$\pm 1/2, e_{\perp}$
$\frac{1}{\sqrt{6}} (111111)$	0	$\frac{2}{3} a^2$	$\frac{8}{9} a^2$	$\frac{2}{9} a^2$
$\frac{1}{2} (11\bar{1}\bar{1}00)$	$\frac{2}{3} b^2$	$\frac{1}{3} b^2$	$\frac{2}{9} b^2$	$\frac{1}{9} b^2$
$\frac{1}{2\sqrt{3}} (1111\bar{2}\bar{2})$	$\frac{2}{3} b^2$	$\frac{1}{3} b^2$	$\frac{2}{9} b^2$	$\frac{7}{9} b^2$
$\frac{1}{\sqrt{2}} (00001\bar{1})$	$\frac{4}{9} \gamma'^2$	$\frac{2}{3} \gamma'^2$	$\frac{4}{3} \gamma'^2$	$\frac{2}{3} \gamma'^2$
$\frac{1}{\sqrt{2}} (1\bar{1}0000)$	$\frac{4}{9} \gamma'^2$	$2 \gamma'^2$	$\frac{4}{3} \gamma'^2$	$\frac{2}{3} \gamma'^2$
$\frac{1}{\sqrt{2}} (001\bar{1}00)$	$\frac{4}{9} \gamma'^2$	$\frac{2}{3} \gamma'^2$	$\frac{4}{3} \gamma'^2$	$\frac{2}{3} \gamma'^2$

Remark.  $e_{\parallel}$  and  $e_{\perp}$  are the polarization vectors for RR directed perpendicular and parallel to [111];  $\mathbf{a} = (2\eta' + \lambda')$ ,  $\mathbf{b} = (\eta'G\lambda')$ .

for compression along the [001] direction and

$$\begin{aligned}
 |\psi_1^A\rangle &= \frac{1}{\sqrt{6}} \left\{ (1+i) \left| \frac{3}{2} \right\rangle - i\sqrt{3} \left| \frac{1}{2} \right\rangle - \left| -\frac{3}{2} \right\rangle \right\}, \\
 |\psi_2^A\rangle &= \bar{K} |\psi_1^A\rangle, \\
 |\psi_3^A\rangle &= \frac{1}{\sqrt{6}} \left\{ (1+i) \left| \frac{3}{2} \right\rangle + i\sqrt{3} \left| \frac{1}{2} \right\rangle - \left| -\frac{3}{2} \right\rangle \right\}, \\
 |\psi_4^A\rangle &= \bar{K} |\psi_3^A\rangle
 \end{aligned} \quad (3)$$

for compression along the [111] direction. The functions  $\psi_1^A, \psi_2^A$  and  $\psi_3^A, \psi_4^A$  form a space which includes functions with angular momentum projections along the [111] direction of  $\pm 1/2$  and  $\pm 3/2$ , respectively. The expressions for the relative decay probabilities for BEs given in Tables II, III depend on the three parameters  $\lambda', \eta',$  and  $\gamma'$  and do not depend on the specific form of the function  $\varphi_m, \psi_m$ .

Let us note that the results we have obtained are in contradiction with the calculations carried out in Ref. 3. For example, according to Ref. 3, the radiative decay of BEs found in the  $\Gamma_5^e$ -state is forbidden, and consequently the  $\alpha$ -NP band cannot be composed of more than two luminescence lines. This clearly contradicts Table II and the spectrum of the  $\alpha$ -NP luminescence band for excitons bound to aluminum atoms, for which three luminescence lines are clearly visible (see Ref. 4). In our opinion, this contradiction is related to the fact that in Ref. 3 the assumption was made that the annihilation of electrons and holes takes place only at those points of the Brillouin zone ( $\Delta_5$ ) corresponding to minima of the conduction band.

Tables II, III allow us to synthesize the luminescence spectrum of excitons bound to acceptors. By requiring optimal agreement between the spectra calculated using Tables II, III and experimental spectra, we can determine the values of the parameters  $\lambda', \eta',$  and  $\gamma'$  along with the relative positions of the bound exciton terms  $\Gamma_1^e, \Gamma_3^e$  and  $\Gamma_5^e$ . We recall that the relative positions of these terms are customarily given by two parameters<sup>1</sup>:  $\Delta_1 = E(\Gamma_5) - E(\Gamma_1)$  and

$\Delta_2 = E(\Gamma_3) - E(\Gamma_1)$ , where  $E(\Gamma_i)$  is the energy corresponding to the term  $\Gamma_i$ .

In Fig. 6 we present the calculated RR spectrum for excitons bound to gallium atoms. In calculating the intensity of individual lines in the RR spectrum, we took into account the degree of degeneracy of the initial and final states of the BE and donors. The spectral positions of the peaks and the values of the constants  $\lambda', \eta',$  and  $\gamma'$  were chosen so that the synthesized spectra coincide as well as possible with the luminescence spectra of excitons bound to gallium atoms (see Fig. 2). The shape of the peaks was determined by the instrument function of a Fabry-Perot interferometer

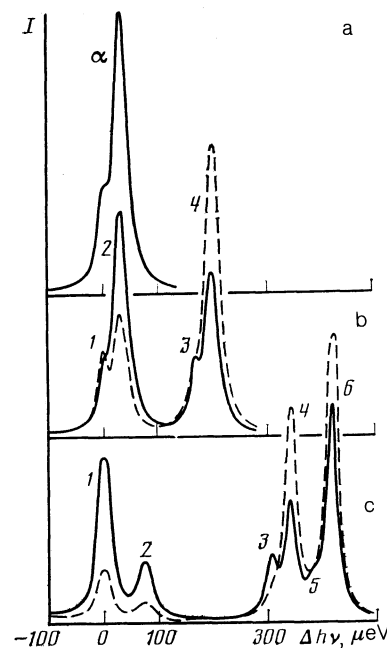


FIG. 6. Calculated spectral distribution of the  $\alpha$ -NP components of the luminescence of excitons bound to impurity atoms of gallium at small stresses. The luminescence is polarized parallel (dotted curve) and perpendicular (continuous curves). The fineness  $F = 25$ ; (a)  $P = 0$ , (b)  $P \parallel [111]$  (c)  $P \parallel [001]$ .

$$I(\delta) = I_0 \left[ 1 + \left( \frac{2}{\pi} F \sin \frac{\delta}{2} \right)^2 \right]^{-1} \quad (4)$$

with fineness  $F$  corresponding to the experimental resolution ( $\delta$  is the phase difference corresponding to two round trips of a beam in the interferometer). In the calculation, the amplitude ratios of the populations of the various BE states are assumed to be different. In addition, we assumed that the wave function of the holes is strongly localized (compared to the electron wave function).<sup>3)</sup> This allowed us to assume the constants  $\lambda$  and  $\lambda'$  were zero (we note that  $\lambda \neq 0$  in the case of impurities of donor type).<sup>1</sup> The depolarization arising from refraction of the RR at the sample surface is taken into account in the following way. According to Table II, peak 1 on Fig. 2 must be fully polarized. However, as can be seen from Fig. 2b,  $I_{\perp} \neq 0$  and ratio  $I_{\parallel}$  to  $I_{\perp}$  comes to 0.3. This disagreement between experiment and theory is connected with RR depolarization. Therefore, in Fig. 6 we present not  $I_{\parallel}$  and  $I_{\perp}$  but rather  $I_{\parallel} = I_{\parallel} + kI_{\perp}$  and  $I_{\perp} = I_{\perp} + kI_{\parallel}$ , where  $k$  is taken to be 0.3 in agreement with Fig. 2b.

From a comparison of the spectra represented by Figs. 2 and 6, it is clear that the disagreement between the experimental and calculated amplitude ratios is insignificant. The parameters determined in this way for excitons bound on gallium atoms equal  $\Delta_1 = -13 \mu\text{eV}$ ,  $\Delta_2 = -42 \mu\text{eV}$  and  $\eta'/\gamma' \approx 1$ . We used these parameters in setting up the level scheme shown in Fig. 5.

The analysis is simpler for the luminescence spectra of excitons bound to impurity atoms of aluminum. This is because in this case all three RR peaks in the spectrum are well separated (see Fig. 4a). So as to identify peaks 1–3 in Fig. 4a, we investigated the RR polarization for samples subjected to compression along the [111] direction. The characteristic RR spectrum for such a sample deformation is presented in Fig. 4b. The degrees of polarization of peaks 1–6 in Fig. 4b equal 19, –24, –64, –40, 32, and 55%, respectively. These values for the degree of polarization agree satisfactorily with the calculated values: 33, –43, –100, –43, 33, and 60%, if it is assumed that the ground state of excitons bound to aluminum atoms is split according to the level scheme shown in Fig. 4. In calculating the degrees of polarization, the intensities corresponding to the transitions 1–6 in Fig. 4 are taken from Table II. We note that when the

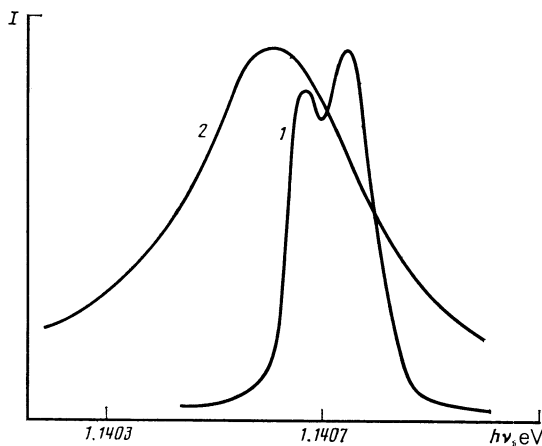


FIG. 7. Spectral distribution of the  $\alpha$ -NP components of the luminescence of excitons bound to impurity atoms of indium in silicon ( $N_{\text{in}} = 7 \times 10^{15} \text{ cm}^{-3}$ ); curve 1— $T = 4.2 \text{ K}$ , the spectral resolution is  $22 \mu\text{eV}$ ; 2— $T = 18 \text{ K}$ , the spectral resolution is  $55 \mu\text{eV}$ .

samples are compressed along the [111] direction the degree of polarization does not depend on the constants which enter into the expressions for the intensities of the RR lines. From the spectra given in Fig. 4a, it is not difficult now to determine the values of the constants  $\Delta_1$  and  $\Delta_2$ , which equal –83 and –108  $\mu\text{eV}$ , respectively.

Furthermore, it follows from Table III that the intensity ratio  $I_1/I_3$  of the RR lines corresponding to the transitions 1 and 3 in Fig. 4 (for  $P = 0$  and  $\lambda = 0$ ) must equal 1/2. The experimental value of  $I_1/I_3$  (see Fig. 4a) equals 2, which differs significantly from the calculated value. However, in the absorption spectrum<sup>3</sup> this ratio is close to the calculated one. The difference between the absorption and luminescence spectra can be explained if we assume that the occupation of the  $\Gamma_3$  state for excitons bound to aluminum atoms is larger than the occupation of the  $\Gamma_1$  state. It is necessary to note that the lack of agreement between experiment and theory can be eliminated if we assume that  $\lambda' \neq 0$ . Then for  $\lambda'/\eta' = -0.5$  and  $\gamma'/\eta' = 1$ , the experimental spectra will be practically indistinguishable from the calculated spectra. However, such an assumption seems counterintuitive to us, because in this case it would be necessary to assume that the probability for interband radiative transitions at the center of the Brillouin zone is several orders of magnitude larger than for  $\mathbf{k}$  corresponding to the bottom of the conduction band.

Let us now consider the RR spectra which arise from radiative decay of excitons bound to impurity atoms of indium in silicon. As is clear from Fig. 7 (spectrum 1), the  $\alpha$ -NP luminescence band for such excitons consists of at least two considerably broadened RR lines separated from one another by approximately  $100 \mu\text{eV}$ . As the sample temperature is varied from 2 to 4.2 K, the shape of the  $\alpha$ -NP band is unchanged. The reason for the broadening of the luminescence lines contained in the  $\alpha$ -NP RR band remains unexplained. This broadening cannot be concentration-dependent, because the latter effect, which we observed, was significant only for  $N_{\text{in}} \sim 10^{17} \text{ cm}^{-3}$ . As the temperature increases above 4.2 K, the band shifts towards longer wavelengths, loses its structure and broadens out. The splitting of the  $\alpha$ -NP RR band we associate with VOS of the BE electron states, because when the crystal is compressed along the [111] direction, this band splits into two equivalent bands, whose origin is the same as for the case of aluminum and gallium. Because of the strong broadening of the RR lines we were unable to determine the  $\Delta_1$  and  $\Delta_2$ .

We are grateful to Ya. E. Pokrovski for valuable advice given during discussion of the results obtained in this paper, and for assistance in carrying it out.

<sup>1)</sup> We have in mind electrons which enter into donors and multiparticle exciton-impurity complexes which include group V elements.

<sup>2)</sup> We recall that the lifetime of a BE in silicon is determined not by radiative but by nonradiative recombination of an electron and hole in the BE.

<sup>3)</sup> It is interesting to note that because of the strong localization of the hole in an exciton bound to an acceptor, the probabilities for radiative decay of the BE into the  $\Gamma_1$  and  $\Gamma_{2,5}$  states must be the same order of magnitude. Actually, in this case the law of quasimomentum conservation is fulfilled because of the hole, and it is unimportant whether or not the amplitude for the electron wave function equals zero at the center. The situation is entirely different for excitons bound to donors, where the

electron is localized. In this case the reduction of the electron wave function to zero at the center (in the states  $\Gamma_{3,5}$ ) sharply reduces the probability for phononless radiative decay of BEs.<sup>1</sup> This leads to a considerable difference in intensities for the  $\Gamma_1$  and  $\Gamma_{3,5}$  lines in the RR spectrum.

<sup>1</sup>V. D. Kulakovski, G. E. Pikus and V. B. Timofeev, *Usp. Fiz. Nauk*, **135**, 237 (1981) [*Sov. Phys. Usp.* **24**, 815 (1981)].

<sup>2</sup>V. A. Karasyuk and Ya. E. Pokrovski, *Pis'ma Zh. Eksp. Teor. Fiz.* **37**,

537 (1983) [*JETP Lett.* **37**, 640 (1983)].

<sup>3</sup>K. R. Elliot, G. C. Osbourn, D. L. Smith and T. C. McGill, *Phys. Rev.* **B17**, 1808 (1978).

<sup>4</sup>A. S. Kaminski, V. A. Karasyuk and Ya. E. Pokrovski, *Zh. Eksp. Teor. Fiz.* **83**, 2237 (1982) [*Sov. Phys. JETP* **56**, 1295 (1982)].

<sup>5</sup>S. A. Lyon, G. C. Osbourn, D. L. Smith and T. C. McGill, *Solid State Commun.* **23**, 425 (1977).

Translated by Frank J. Crowne